

# THE INWARD SOLIDIFICATION OF SPHERES AND CIRCULAR CYLINDERS

D. S. RILEY

Department of Mathematics, University of Southampton

F. T. SMITH

Department of Mathematics, Imperial College, London

and

G. POOTS

Department of Applied Mathematics, University of Hull

(Received 30 October 1973 and in revised form 6 May 1974)

**Abstract**—An analytical study is presented of the inward freezing of a sphere or a circular cylinder, initially molten and at the fusion temperature, when the outside surface is suddenly cooled. The treatment assumes, among other things, constant thermal properties and that the parameter  $\beta$ , the ratio of the latent heat to the sensible heat of the substance, is large. Basic series solutions are first derived and these are then followed by a two-region analysis which is needed to accommodate the sharp change in thermal profile just before the centre of the sphere or the cylinder solidifies. Although the theory is strictly asymptotic in nature, results compare well with numerical solutions of the full problem for  $\beta = 10$  and 20 (cylinder) and  $\beta = 10$  (sphere).

## NOMENCLATURE

$a^*$ , radius of body;  
 $c_p$ , specific heat at constant pressure;  
 $k$ , thermal conductivity;  
 $J_0, J_1$ , Bessel functions of zero- and first-order respectively;  
 $j_n$ , zeros of  $J_0$ ;  
 $L$ , latent heat of fusion;  
 $r^*$ , radial coordinate;  
 $S^*$ , penetration depth;  
 $T^*$ , temperature;  
 $T_D = T_F^* - T_0^*$ , temperature difference;  
 $t^*$ , time;  
 $q, r, s, R, S$ , dimensionless coordinates.

## Affices

0, body wall;  
 $F$ , fusion;  
 $*$ , physical variables; unstarred quantities denote dimensionless variables;  
 $\hat{\phantom{x}}$ , dimensionless variables of region II;  
 $\lambda$ , 1 (cylinder) or 2 (sphere).

## INTRODUCTION

IN THE last few years there has been a considerable upsurge of interest in multiphase processes, which are of particular concern in such diverse fields as refrigeration, thermoplastics, electrochemistry, metal-casting and welding, and geophysics. For example, many theoreticians and experimentalists have recently turned their attention to deep penetration welding, which has an important application in the construction of nuclear power installations.

A feature of these problems is the existence of a moving interface between the phases, at which thermal energy in the form of latent heat is liberated. Unfortunately, the mathematical condition at this interface is non-linear and, in consequence, generalized analytical solutions are not readily available, even for simple geometries. A good number of the works on this topic have been reviewed by Rubinstein [1] and Carslaw and Jaeger [2], but they mostly involve linear heat flows. Investigations involving "finite" geometries have, in general, been made by using numerical techniques.

## Greek symbols

$\beta$ ,  $= \frac{L}{c_p T_D}$ , dimensionless parameter;  
 $\Delta$ , stretching factor of equation (3.1);  
 $\kappa$ , thermal diffusivity;  
 $\rho$ , density;  
 $\eta$ , normalised dimensionless coordinate;  
 $\theta$ ,  $= \frac{T^* - T_0^*}{T_F^* - T_0^*}$ , normalized dimensionless temperature;  
 $\gamma$ , Euler's constant.

In order that further inroads be made into the ever increasingly complex problems occurring in industry, it seems highly desirable to have a general technique for treating them. In this paper it is proposed to treat the problems by perturbation methods, the critical large parameter being

$$\beta = \frac{L}{c_p T_D},$$

the ratio of the latent heat to the heat capacitance of the solidified phase. Here  $L$  is the latent heat of fusion of the substance,  $c_p$  the specific heat and  $T_D$  the temperature difference between the fusion temperature and the outer surface temperature. Therefore, we are concerned with situations where, for example, the temperature difference,  $T_D$ , is small and the latent heat is large (see Table 1).

Table 1

Material	Specific heat, $c_p$ (at 0°C) cal g <sup>-1</sup> °C <sup>-1</sup>	Latent heat of fusion, $L$ cal/g	$(L/c_p)$ °C <sup>-1</sup>
Aluminium	0.2096	96	458.02
Copper	0.0909	49	539.05
Gold	0.0350	15	429.57
Iron	0.1045	64	612.44
Lead	0.0302	6	199.68
Magnesium	0.2460 (18°C)	90	367.85
Mercury	0.0335	2.8	84.58
Nickel	0.1060	73	689.68
Zinc	0.0918	24	261.44

The problems considered here are those of the inward solidification of a circular cylinder and of a sphere, which are initially at the fusion temperature and whose outer surfaces are maintained at a temperature less than that of fusion. Our aim in the analysis is amongst other things to derive a formula determining the time required for the cylinder or sphere to become totally solidified and the temperature profile at that moment.

The majority of investigations dealing specifically with cylinders and spheres are catalogued in the introduction by Tao [3] in his paper on generalized numerical solutions for these problems. Other noteworthy contributions have been made by Poots [4], who found short-time solutions, and Beckett [5] who extended Poots' analysis and also found numerical solutions employing the Hartree-Wormersley technique. More recently, Pedroso and Domoto [6, 7] developed perturbation solutions for the sphere problem and modified the resulting series, which are divergent at the centre of the sphere, by means described in Section 2.

The major simplifying assumptions made are that the melt is always at its fusion temperature and that there exists at all times a sharply-defined line of

division, the solidification front, between the solid and the liquid (the latter being a good approximation especially for pure metals). These assumptions enable straightforward perturbation solutions for the temperature and the inward travel of the front to be derived. This particular work has been carried out by Pedroso and Domoto [6] for the sphere and by Riley [8] for the cylinder and for convenience we restate their results in Section 2. The instant at which total solidification is attained represents a singularity in the straightforward approach, and this we set out to treat by an expansion theory strictly valid only for  $\beta \gg 1$ . We discover in Section 3 that when the interface is close to the centre, the features of the heat flow take on quite different forms in two terminal regions, one near the interface which is controlled by the latent heat condition and the other further out where (in contrast with the original solution) the variation of temperature with time plays a key part in fixing the final development of the solidification front. Our solutions are compared with Tao's [3] results for the sphere for  $\beta = 10$ , and with Beckett's [5] results for the cylinder for  $\beta = 10$  and 20.

## 2. THE GOVERNING EQUATIONS AND BASIC PERTURBATION SOLUTION

The two problems under consideration in this paper are summarized in Fig. 1. Initially the material within

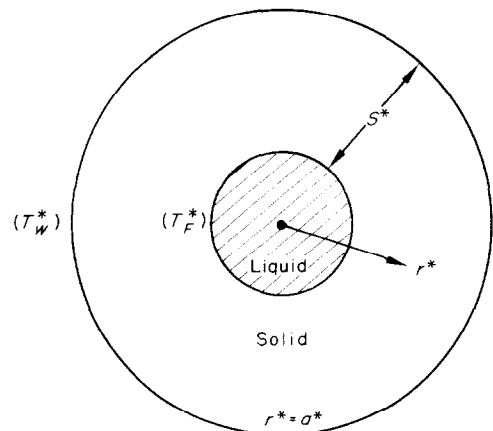


FIG. 1. The spherical or cylindrical configuration for the inward-travelling solidification front.

the spherical or cylindrical body  $0 \leq r^* \leq a^*$  is completely molten and at its uniform fusion temperature  $T_f^*$ , but at time  $t^* = 0$  a lower constant temperature  $T_w^*$  is suddenly imposed, and thereafter maintained, at the surface  $r^* = a^*$ , which causes the body subsequently to solidify inwards. The radial distance of the solid/melt interface from the surface  $r^* = a^*$  at time  $t^* \geq 0$  will be denoted by  $S^*(t^*)$  and we shall suppose that the molten

part of the sphere or cylinder always remains at the fusion temperature, while the flow of heat through the solidified part is purely radial.

For both geometries suitable non-dimensional variables are obtained by writing

$$S = \frac{S^*}{a^*}, \quad \theta = \frac{T^* - T_w^*}{T_f^* - T_w^*}, \quad R = \frac{r^*}{a^*}, \quad \tau = \frac{\kappa t^*}{\beta a^{*2}} \quad (2.1)$$

where

$$\beta = \frac{L}{c_p(T_f^* - T_w^*)}, \quad (2.2)$$

$T^*$  is the temperature of the solid state and  $\kappa$  its thermal diffusivity. Further, it proves to be convenient to consider  $\tau$  as a function of  $S$ , with  $\theta$  depending on the independent variables  $R, S$  (see Riley [8]); the variation of temperature within the solidified material is then described by the heat-conduction equation in the form

$$\left( \frac{\partial^2}{\partial R^2} + \frac{\lambda}{R} \frac{\partial}{\partial R} \right) \theta = \frac{1}{\beta} \frac{\partial \theta}{\partial S} / \tau'(S) \quad (2.3)$$

for  $\lambda = 1$  (the cylinder) or  $\lambda = 2$  (the sphere), subject to the boundary conditions

$$\theta = 0 \text{ at } R = 1, \quad \theta = 1 \text{ at } R = 1 - S \quad (2.4)$$

$$\frac{\partial \theta}{\partial R} = -\frac{dS}{d\tau} \text{ at } R = 1 - S \quad (2.5)$$

and the obvious initial conditions. Equation (2.5) expresses the usual latent heat condition based on an energy balance at the solidification front. The two major advantages of the prescription (2.3–2.5) are that the front is set permanently at one end of the region of interest, and the total solidification time  $\tau_f$ , i.e. the instant at which the solidification front reaches the centre,  $r^* = 0$ , and the associated (terminal) temperature distribution  $\theta_f(R)$ , are given precisely by  $\tau_f = \tau(S = 1)$  and  $\theta_f(R) = \theta(S = 1)$ .

The sole fundamental parameter is  $\beta$ , and in the remainder of our discussion we shall suppose that

$$\beta \gg 1 \quad (2.6)$$

(see Section 1) and seek an asymptotic solution. We begin by expanding the temperature field and time in straightforward fashion:

$$\theta = \theta_0 + \frac{1}{\beta} \theta_1 + \frac{1}{\beta^2} \theta_2 + \dots \quad (2.7)$$

$$\tau = \tau_0 + \frac{1}{\beta} \tau_1 + \frac{1}{\beta^2} \tau_2 + \dots \quad (2.8)$$

and substituting into (2.3–2.5) along with the appropriate initial constraints. The time-dependence is thereby relegated to a secondary rôle. In principle as many terms of the series as we please may be calculated, and we quote the results:

for  $\lambda = 2$  (sphere),

$$\begin{aligned} \theta = & \frac{(1-S)(1-R)}{RS} \\ & + \frac{(1-R)}{6\beta(1-S)RS} \left\{ 1 - \left( \frac{1-R}{S} \right)^2 \right\} - \frac{(1-R)}{\beta^2(1-S)^3 RS} \\ & \times \left\{ \frac{1}{36} \left[ 1 - \left( \frac{1-R}{S} \right)^2 \right] + \left( \frac{3-4S}{120} \right) \left[ 1 - \left( \frac{1-R}{S} \right)^4 \right] \right\} \\ & + O(\beta^{-3}) \end{aligned} \quad (2.9a)$$

$$\tau = \frac{3S^2 - 2S^3}{6} + \frac{S^2}{6\beta} - \frac{S^2}{45\beta^2(1-S)} + O(\beta^{-3}) \quad (2.9b)$$

(due to Pedroso and Domoto [9]);

for  $\lambda = 1$  (cylinder), setting  $\eta = \frac{1-R}{S}$

$$\begin{aligned} \theta = & \frac{\ln(1-S\eta)}{\ln(1-S)} \\ & - \left\{ [(1-S\eta)^2 - (1-S)^2] \ln(1-S\eta) + 1 \right. \\ & \left. - (1-S\eta)^2 + [(1-S)^2 - 1] \frac{\ln(1-S\eta)}{\ln(1-S)} \right\} / \\ & \{ 4\beta(1-S)^3 \ln^2(1-S) \} + O(\beta^{-2}) \end{aligned} \quad (2.10a)$$

$$\begin{aligned} \tau = & \frac{1}{4} \{ (1-S)^2 [\ln^2(1-S) - 1] + 1 \} \\ & + \frac{1}{4\beta} \left\{ \frac{1 - (1-S)^2}{\ln(1-S)} + 1 + (1-S)^2 \right\} + O(\beta^{-2}) \end{aligned} \quad (2.10b)$$

(due to Riley [12], who also gives the  $O(\beta^{-2})$  terms in (2.10)). For small  $S$  the results are identical with the small-time solutions for any  $\beta$  found by Poots [4].

No information is given, however, on the thermal properties at solidification for, as the interface nears the centre ( $\tau \rightarrow \tau_f, S \rightarrow 1$ ), not only does the accuracy of the approximation routine (2.7–2.8) deteriorate but the expansions for  $\theta$  and  $\tau$  break down. Therefore compensatory measures must be taken, particularly for some range  $0 \leq 1 - S \ll 1$ , to remove the singularities at  $S = 1$  in the straightforward scheme. With this in mind Pedroso and Domoto [6, 7], for  $\lambda = 2$ , used an Euler transformation and an adaptation of the strained coordinates method incorporating a Shanks transformation to force the time-variation to be reasonably well-behaved at  $S = 1$ , but the methods do not for instance bring out all the physics of the problem and we suggest that our approach, employing a rational matched expansion theory, is more enlightening as well as systematic since it provides both physical and mathematical insight into the essential nature of the freezing process near the centre. Consequently, from an inspection of the singular expansions (2.9–2.10), we shall now deduce the new form that the process develops in the vicinity of the terminal station  $S = 1$  for  $\lambda = 1$  and  $\lambda = 2$ .

3. THE NEW STRUCTURE NEAR COMPLETE SOLIDIFICATION

Near the centre the substitution

$$S = 1 - \Delta_\lambda s \tag{3.1}$$

is appropriate, where  $s = O(1)$  defines the region of invalidity of (2.9–2.10) and the factor  $\Delta_\lambda \ll 1$  is to be determined for each  $\lambda = 1, 2$ .

(a) *The sphere*

Putting (3.1) into (2.9b) implies that the second term in  $\tau'(S)$  overtakes the leading one when  $\Delta_2 \sim \beta^{-1/2}$ , so that (2.9b) is then incorrect, and the same estimate is provided by (2.9a). However the temperature field also takes on quite different characteristics when  $R$  is of  $O(1)$  and when  $R$  is of  $O(\Delta_2)$ , under (3.1), and we may surmise that the heat-flow should be examined in two separate regions when

$$\Delta_2 = \beta^{-1/2}. \tag{3.2}$$

Starting in the first domain, region I, the new expansions stemming from (2.9a–b) are

$$\begin{aligned} \theta &= T_0 + \beta^{-1/2} T_1 + \beta^{-1} T_2 + O(\beta^{-3/2}) \\ \tau &= \frac{1}{6} + \frac{t_0(s)}{\beta} + \frac{t_1(s)}{\beta^{3/2}} + \frac{t_2(s)}{\beta^2} + O(\beta^{-5/2}) \end{aligned} \tag{3.3}$$

for  $s$  and  $r$  of  $O(1)$ , where

$$r = \beta^{-1/2} R$$

with the boundary conditions that  $\theta = 1$  on  $r = s$ , the latent-heat balance:

on  $r = s$ ,

$$\begin{aligned} \frac{\partial}{\partial r} \{T_0 + \beta^{-1/2} T_1 + \dots\} \\ = \frac{1}{t_0(s)} \left\{ 1 - \beta^{-1/2} \frac{t'_1}{t_0} + \beta^{-1} \left( \frac{t_1'^2 - t_0' t_2'}{t_0^2} \right) + \dots \right\} \end{aligned} \tag{3.4}$$

and matching to the basic scheme (2.9) as  $s \rightarrow \infty$ , with  $r \sim s$ , and to region II (see below) as  $r \rightarrow \infty$  with  $s$  fixed. Substituting (3.3) into (2.3) with  $\lambda = 2$  and equating terms of equal order in  $\beta^{-1}$ , the solutions satisfying the interface conditions are found to be

$$\begin{aligned} T_0 &= 1 + B_0(s) \left( \frac{1}{r} - \frac{1}{s} \right), \quad T_1 = B_1(s) \left( \frac{1}{r} - \frac{1}{s} \right) \\ T_2 &= \left( \frac{B_0 - s B_0'}{6s^2 t_0'} \right) (r^2 - s^2) + \frac{B_0'}{2t_0'} (r - s) + B_2(s) \left( \frac{1}{r} - \frac{1}{s} \right) \end{aligned}$$

where

$$\begin{aligned} B_0 &= \frac{-s^2}{t_0'}, \quad B_1 = \frac{s^2 t_1'}{t_0'^2}, \\ B_2 &= \frac{s}{6t_0'^3} (2B_0 + s B_0' + 6t_0' t_2' - 6t_1'^2). \end{aligned}$$

Further,  $\tau$  in (3.3) must approach (2.9b) as  $s \rightarrow \infty$ , which imposes

$$\begin{aligned} t_0 &\sim \frac{1 - 3s^2}{6}, \quad t_1 \sim \frac{s^3 - s}{3} - \frac{1}{45s} + O(s^{-3}), \\ t_2 &\sim \frac{s^2}{6} + \frac{2}{45} + O(s^{-2}) \quad \text{as } s \rightarrow \infty \end{aligned} \tag{3.5}$$

and also secures the merging between  $\theta$  in (3.3) and (2.9a). Anticipating the match with region II, we then have that, as  $r \rightarrow \infty$  in I, the temperature takes on the form

$$\begin{aligned} \theta &\sim \left\{ \left( \frac{B_0}{s} - 1 \right) + \frac{s^2 R^2}{6B_0} \left( \frac{B_0}{s} \right)' + O(R^3) \right\} \\ &+ \beta^{-1/2} \left\{ \frac{B_0}{R} - \frac{B_1}{s} - \frac{B_0 B_0' R}{2s^2} + O(R^2) \right\} \\ &+ \beta^{-1} \left\{ \frac{B_1}{R} - \left( \frac{B_0 + 2B_0'}{6t_0'} + \frac{B_2}{s} \right) + O(R) \right\} \\ &+ O(\beta^{-3/2}). \end{aligned} \tag{3.6}$$

In region II, which is required to continue from I, i.e. from (3.6), out to  $R = 1$ , both (3.6) and (2.9a) indicate that  $R$  itself is the relevant radial coordinate and that

$$\theta = \beta^{-1/2} \hat{T}_0 + \beta^{-1} \hat{T}_1 + O(\beta^{-3/2}) \tag{3.7}$$

should be set. We now attempt to comply with the surface condition

$$\hat{T}_0 = \hat{T}_1 = \dots = 0 \quad \text{at } R = 1 \tag{3.8}$$

as well as joining to I when  $R \rightarrow 0$  and to (2.9a) when  $s \rightarrow \infty$  for  $0 < R \leq 1$ . Upon insertion of (3.7) into the full equation (2.3), terms  $O(\beta^{-1/2})$  give

$$\left( \frac{\partial^2}{\partial R^2} + \frac{2}{R} \frac{\partial}{\partial R} \right) \hat{T}_0 = \frac{1}{t_0'} \frac{\partial \hat{T}_0}{\partial s} \tag{3.9}$$

while consistency between (3.6) and (3.7) as  $R \rightarrow 0$  demands that

$$B_0(s) = s, \quad t_0(s) = \frac{1}{6} (1 - 3s^2), \quad T_0 = \frac{s}{r}$$

and

$$\hat{T}_0 \sim \frac{s}{R} - \frac{t_1'(s)}{s} + O(R) \quad \text{as } R \rightarrow 0. \tag{3.10}$$

Finally, matching with (2.9a) imposes

$$\begin{aligned} \hat{T}_0 &\sim s \left( \frac{1-R}{R} \right) + \left( \frac{1-R}{6sR} \right) [1 - (1-R)^2] + \left( \frac{1-R}{Rs^3} \right) \\ &\times \left\{ \frac{1}{36} [1 - (1-R)^2] - \frac{1}{120} [1 - (1-R)^4] \right\} + \dots \\ &\quad \text{as } s \rightarrow \infty. \end{aligned} \tag{3.11}$$

Hence the heat flow in II is dictated by the closed problem (3.8)–(3.11) for  $\hat{T}_0$ .

(b) *The cylinder*

Under (3.1) we now find that the value of  $\Delta_1 \ll 1$  which first renders (2.10a, b) invalid is given by

$$\Delta_1^2 \ln \Delta_1 = \frac{-1}{\beta} \tag{3.12}$$

and that again there is a pronounced distinction between the behaviour of  $\theta$  near the interface ( $\eta \sim 1$ ) and further out ( $1-\eta \sim 1$ ) as  $S \rightarrow 1$ , which leads to the following two-tiered approach.

In the inner region I, where now

$$r = \frac{1-\eta}{\Delta_1}$$

and  $s$  are  $O(1)$ , the temperature and time variations develop in the forms

$$\begin{aligned} \theta &= 1 + \frac{T_1}{\ln \Delta_1} + \frac{T_2}{(\ln \Delta_1)_2} + \dots \\ \tau &= \frac{1}{4} - \frac{t_1(s)}{\beta} - \frac{t_2(s)}{\beta(\ln \Delta_1)} - \frac{t_3(s)}{\beta(\ln \Delta_1)^2} - \dots \end{aligned} \tag{3.13}$$

subject to the interface conditions at  $r = 0$ , matching with (2.10) as  $s \rightarrow \infty$  (with  $r \sim s$ ) and with region II below as  $r \rightarrow \infty$ . The heat-flow equation with  $\lambda = 1$  then produces the solutions

$$T_i = A_i(s) \ln \left( 1 + \frac{r}{s} \right) \quad \text{for } i = 1, 2, \dots$$

where

$$\frac{A_1}{s} = \frac{1}{t'_1}, \quad \frac{A_2}{s} = \frac{-t'_2}{t_1'^2}, \quad \frac{A_3}{s} = \frac{t_2'^2 - t_1' t_3'}{t_1'^3}$$

and as  $s \rightarrow \infty$ ,

$$\begin{aligned} t_1 &\sim \frac{s^2}{2} - \frac{1}{4}, \quad t_2 \sim \frac{s^2}{2} \ln s - \frac{s^2}{4} - \frac{1}{4} \\ t_3 &\sim \frac{1}{4} \ln s + \frac{5}{128s^2} + O(s^{-4}). \end{aligned}$$

Moving on to region II in which  $\eta$  and  $s$  are the independent variables, we set

$$\theta = \frac{\hat{T}_1}{\ln \Delta_1} + \frac{\hat{T}_2}{(\ln \Delta_1)^2} + O((\ln \Delta_1)^{-3}) \tag{3.14}$$

as implied by (2.10a) and (3.13). Terms of equal order in  $\beta^{-1}$  in the heat-flow equation then give

$$\begin{aligned} \frac{\partial^2 \hat{T}_1}{\partial \eta^2} - \left( \frac{1}{1-\eta} \right) \frac{\partial \hat{T}_1}{\partial \eta} &= \frac{-1}{t'_1} \frac{\partial \hat{T}_1}{\partial s} \\ \frac{\partial^2 \hat{T}_2}{\partial \eta^2} - \left( \frac{1}{1-\eta} \right) \frac{\partial \hat{T}_2}{\partial \eta} &= \frac{-1}{t'_1} \frac{\partial \hat{T}_2}{\partial s} + \frac{t'_2}{t_1'^2} \frac{\partial \hat{T}_1}{\partial s} \end{aligned} \tag{3.15}$$

with the boundary conditions

$$\begin{aligned} \text{at } \eta = 0, \quad \hat{T}_1 &= \hat{T}_2 = 0 \\ \text{as } s \rightarrow \infty, \quad \hat{T}_1 &\rightarrow \ln(1-\eta) \end{aligned}$$

$$\begin{aligned} \hat{T}_2 &\sim -\ln s \ln(1-\eta) \\ &+ \frac{1}{4s^2} \{ 1 - (1-\eta)^2 + (1-\eta)^2 \ln(1-\eta) \} \\ &+ \frac{1}{64s^2} \{ 8(1-\eta)^2 - 3(1-\eta)^4 \\ &+ 2(1-\eta)^4 \ln(1-\eta) - 5 \} + \dots \end{aligned} \tag{3.17}$$

to merge with (2.10a), and lastly we require agreement with region I near  $\eta = 1$ . Rearrangement of  $\theta$  in (3.17) for  $r \gg 1$  shows however that, for this last requirement to hold,

$$A_1(s) = 1, \quad t_1(s) = \frac{s^2}{2} - \frac{1}{4}, \quad \hat{T}_1 = \ln(1-\eta),$$

$$A_2(s) = -\ln s, \quad t_2(s) = \frac{1}{2} s^2 \ln s - \frac{s^2}{4} + \frac{1}{4}$$

and

$$\hat{T}_2 \sim -\ln s \ln(1-\eta) + \frac{1}{s} t_3'(s) + o(1) \quad \text{as } \eta \rightarrow 1^- \tag{3.18}$$

Therefore we are left with the closed problem (3.15–3.18) controlling both the secondary heat-flow  $\hat{T}_2$  and the time-factor  $t_3(s)$ .

The fundamental problems arrived at in (a) and (b) will be solved in Section 4 below. However, before moving on to the solution we feel a few further comments concerning the new double-structure are worthy of note. First, from the physical standpoint we observe that, except in the close neighbourhood of the solid-liquid interface, the temporal dependence of the temperature within the solidified material cannot be neglected in the final stages of the solidification even though the latent heat parameter  $\beta$  is large. For the righthand sides of (3.9) and (3.15) are effectively time-variations written in the  $S$ - $R$  coordinate system. Thus, although the time-dependent factor in the heat flow has a relatively small influence during most of the process, its effect accumulates and becomes of the same order of magnitude as the spatial-dependence when the actual distance of the interface from the centre is as small as  $a\Delta_\lambda$ , explaining why at that stage the supplementary expansions in I and II are required and the temporal variation is retained in the governing equations (3.9), (3.15). Second, examination of the scalings shows that it is not enough to consider one region on its own when  $(1-S)$  is of order  $\Delta_\lambda$ . The inner region I provides for a proper appreciation of the latent-heat condition at the front, while region II (where the temperature is an order of magnitude lower than in I) is needed to account for the prime importance

of the time dependence throughout the major part of the body as well as allowing for the condition at the surface  $r^* = a^*$ .

4. SOLUTION OF THE TERMINAL PROBLEMS

The essential problems near complete freezing, as stated in Section 3 (a) and (b), are amenable to treatments by transform methods. For convenience we write

$$q = s^2. \tag{4.1}$$

(a) *The sphere*

Putting  $\hat{T}_0 = F/R$  and  $R = 1 - x$ , we define the finite Fourier sine-transform of  $F$ :

$$\bar{F} = \int_0^1 F(x, q) \sin n\pi x \, dx. \tag{4.2}$$

Equation (3.9) and the conditions at  $x = 0, 1$  yield the solution

$$\bar{F} = (-1)^n \frac{n\pi}{2} e^{n^2\pi^2q/2} \left\{ A + \int_0^q q_1^{1/2} e^{-n^2\pi^2q_1/2} \, dq_1 \right\},$$

the constraint (3.11) then implies  $A = 0$  and thence, taking the inverse of (4.2), we obtain the Fourier series solution

$$F(x, q) = 2(\sqrt{2}) \sum_1^\infty \frac{(-1)^n}{n^2\pi^2} e^{n^2\pi^2q/2} \Gamma\left(\frac{3}{2}, \frac{n^2\pi^2q}{2}\right) \sin n\pi x \tag{4.3}$$

where  $\Gamma$  is the incomplete gamma function. On integration (3.10) now gives

$$t_1 - \frac{1}{3}q^{3/2} + \frac{1}{3}q^{1/2} = -\left(\frac{2}{\pi^5}\right)^{1/2} \sum_1^\infty \frac{e^{n^2\pi^2q/2}}{n^3} \operatorname{erfc}(n\pi \sqrt{q/2})$$

with  $\operatorname{erfc}$  denoting the complementary error function, and so when the sphere is completely solidified

$$t_1 = t_1(0) = -\left(\frac{2}{\pi^5}\right)^{1/2} \sum_1^\infty \frac{1}{n^3} = \frac{-1}{3(2\pi)^{1/2}}$$

or from (3.3) the total solidification time is

$$\tau_f = \frac{1}{6} + \frac{1}{6\beta} - \frac{1}{3(2\pi)^{1/2}\beta^{3/2}} + O(\beta^{-2}). \tag{4.4}$$

Correspondingly the final temperature profile comes from

$$F(x, 0) = -\left(\frac{2}{\pi^3}\right)^{1/2} \sum_1^\infty \frac{(-1)^n}{n^2} \sin n\pi x = -\left(\frac{2}{\pi^3}\right)^{1/2} f(\pi R)$$

where

$$f(\pi R) = -\int_0^{\pi R} \ln(2 \sin \frac{1}{2}t) \, dt \tag{4.5}$$

is Clausen's Integral (Abramowitz and Stegan [9], p. 1005), so that to first order

$$\theta_f(R) = \beta^{-1/2} \hat{T}_0(x, 0) = \left(\frac{2}{\pi^3\beta}\right)^{1/2} \frac{f(\pi R)}{R}. \tag{4.6a}$$

We remark that (4.6a) has a logarithmic growth as  $R \rightarrow 0$ .

Partly to confirm the consistency of the terminal structure envisaged in Section 3(a) but more especially for the purpose of bettering the accuracy of  $\theta_f(R)$  for moderate values of  $\beta$ , we have taken the analysis of zone II one step further by working out the second order term  $\hat{T}_1$  of expansion (3.7). Application of the matching techniques employed previously shows that  $\hat{T}_1$  must satisfy

$$\left(\frac{\partial^2}{\partial R^2} + \frac{2}{R} \frac{\partial}{\partial R}\right) \hat{T}_1 = \frac{-1}{s} \frac{\partial \hat{T}_1}{\partial s} - \frac{t_1'(s)}{s^2} \frac{\partial \hat{T}_0}{\partial s}$$

and

$$\hat{T}_1 \sim \frac{t_1'(s)}{R} + \left[ \frac{1}{2} + \frac{1}{2s^2} - \frac{t_2'(s)}{s^2} - \frac{(t_1'(s))^2}{s^2} \right] + o(1) \text{ as } R \rightarrow 0$$

$$\hat{T}_1 = 0 \text{ at } R = 1$$

$$\hat{T}_1 \sim s^2 \left(\frac{1}{R} - 1\right) + \left(\frac{1-R}{6R}\right) [1 - 3(1-R)^2] + O(s^{-2}) \text{ as } s \rightarrow \infty.$$

By using the Fourier sine transform and pursuing a course of action akin to that for  $\hat{T}_0$ ,  $\hat{T}_1$  is determined implicitly by  $\hat{T}_1 = F_1/R$  and

$$\bar{F}_1 = \sum_{m=1}^\infty (-1)^n \frac{m^2 n^3 \pi^5}{4} \times \int_q^\infty e^{m^2\pi^2u/2} \Gamma\left(\frac{3}{2}, \frac{n^2\pi^2u}{2}\right) \Gamma\left(\frac{3}{2}, \frac{m^2\pi^2u}{2}\right) \, du \tag{4.7}$$

where the bar denotes the transform. The most significant result from (4.7) would obviously be an explicit formula for  $\hat{T}_1(R, 0)$  but unfortunately we have so far been unable to express the inverse of (4.7), even at  $q = s = 0$ , in anything more concise than a double series form, despite several different approaches to the problem (details of which are omitted). On the other hand a reasonable estimate of the behaviour of  $\hat{T}_1(R, 0)$  may be obtained by retaining in the series (4.7) only the terms for which  $m = n$ ; the correction to the terminal profile (4.6a) then comes out at

$$\frac{1}{\beta} \hat{T}_1(R, 0) = \left(\frac{3\pi - 32}{18\beta}\right) (2 - 3R + R^2) \text{ [estimate]} \tag{4.6b}$$

(b) *The cylinder*

Putting  $x = 1 - \eta$  and using the known results for  $t_1$  and  $T_1$ , (3.15) becomes

$$\frac{1}{x} \frac{\partial}{\partial x} \left( x \frac{\partial \hat{T}_2}{\partial x} \right) = -2 \frac{\partial \hat{T}_2}{\partial q}. \tag{4.7}$$

Applying the finite Hankel transform

$$T_n = \int_0^1 x J_0(j_n x) \hat{T}_2(x, q) \cdot \frac{2}{[J_1(j_n)]^2} \, dx$$

with  $j_n$  denoting the zeros of the zero-order Bessel function  $J_0(Z)$  and  $J_1(Z)$  being the Bessel function of

first order, we find the solution of (4.7), satisfying the conditions at  $x = 0, 1$ , to be

$$T_n = e^{i^2 q/2} \int_0^q e^{-i^2 u/2} \ln u \, du \cdot \frac{-1}{2[J_1(j_n)]^2}$$

which also recovers (3.17) precisely. Hence  $\hat{T}_2$  is determined as the Fourier-Bessel series

$$\hat{T}_2 = \sum_1^\infty T_n(q) J_0(j_n x) \tag{4.8}$$

from which the following contribution to the terminal temperature profile ( $q = 0$ ) is obtained:

$$\frac{\hat{T}_2(x, 0)}{(\ln \Delta_1)^2} = \frac{1}{2(\ln \Delta_1)^2} \left[ (\gamma - \ln 2) \ln x - 4 \sum_1^\infty \frac{J_0(j_n x) \ln j_n}{[J_1(j_n)]^2 j_n^2} \right] \tag{4.9}$$

The derivative of the temporal distribution  $t_3(q)$  is now given by the finite part of (4.8) at  $x = 0$ . Therefore

$$t_3(q) = \frac{1}{2} \sum_1^\infty \frac{e^{i^2 q/2}}{[J_1(j_n)]^2 j_n^2} \int_0^q e^{-i^2 u/2} \ln u \, du \tag{4.10}$$

and we deduce that the resultant contribution to the total solidification time  $\tau_f$  is

$$\frac{-t_3(0)}{\beta(\ln \Delta_1)^2} = \frac{1}{\beta(\ln \Delta_1)^2} \left[ \left( \frac{\gamma - \ln 2}{8} \right) + 2 \sum_1^\infty \frac{\ln j_n}{[J_1(j_n)]^2 j_n^4} \right] \tag{4.11}$$

5. RESULTS AND DISCUSSION

For the sphere the travel of the solid-melt interface towards the centre and the terminal temperature distribution  $\theta_f(R)$  of (4.6a, b) are depicted in Fig. 2, along

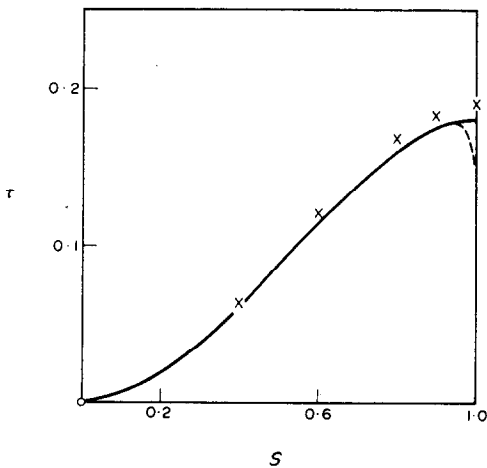


FIG. 2(a). Time  $\tau$  vs front position  $S$  for the sphere when  $\beta = 10$ . The continuous line is the solution including the two-region formula (4.4) near  $S = 1$ , the crosses are Tao's [3] numerical results and the dashed curve indicates the inefficiency of the original series (2.9b).

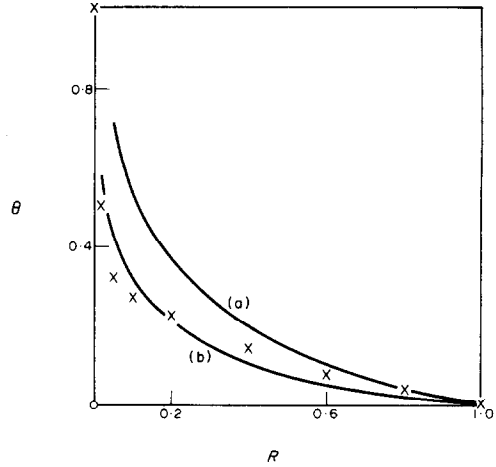


FIG. 2(b). Comparison for  $\beta = 10$  between the terminal temperature profiles computed by Tao [3] and those due to (a) the one-term result (4.6a), (b) the two-term formula incorporating the estimated correction (4.6b).

with Tao's [3] computed results, when  $\beta = 10$ . Remembering that the relative error in the theory is  $O(\beta^{-1/2})$ , or about 0.3 in this case, the agreement is satisfactory, and it is interesting to note that if the logarithmic growth  $\ln \pi R$  in (4.6a) is subtracted off for all values of  $R$  then the agreement from just the one-term formula (4.6a) is improved over the entire range.

For the cylinder, in order to gauge the applicability of our  $\beta \gg 1$  analysis for moderate values of  $\beta$ , graphs of Beckett's [5] numerical results for  $\beta = 10, 20$  are drawn in Fig. 3 for reference. They agree, incidentally, with the work of Allen and Severn [10] and Tao [3] within the limits of graphical accuracy, except in the vicinity of the centre where they are believed to be more accurate. For the same  $\beta$ 's the solutions given by the basic series (2.10a) are displayed in Fig. 4, together with the final temperature distribution derived from the two-region examination, namely

$$\theta_f(R) = \frac{\ln R}{\ln \Delta_1} - \frac{1}{2(\ln \Delta_1)^2} \times \left\{ (\ln 2 - \gamma) \ln R + 4 \sum_1^\infty \frac{J_0(j_n R) \ln j_n}{[J_1(j_n)]^2 j_n^2} \right\} \tag{5.1}$$

although, to be precise, only the first ten terms of (5.1) have been included in Fig. 4. For each  $\beta$ , series (2.10a) is in good agreement with the computed values of Fig. 3 for  $\tau \leq 0.9\tau_f$ , but near total solidification it is necessary to combine (2.10a) with the formula (5.1), and the steep gradient of the thermal profile is then correctly predicted. Figure 5 shows both the computed solutions of Beckett [7] and the results due to the present work (series (2.10b) and the I-II analysis) for the interface position  $S(\tau)$  when  $\beta = 10, 20$ , and here

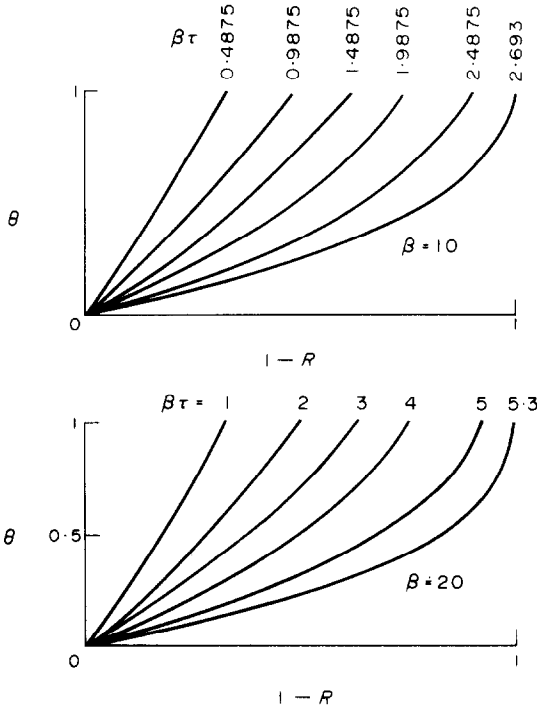


FIG. 3. Temperature distributions during the freezing for  $\beta = 10$  and  $20$ , from Beckett's [5] numerical solutions of the full problem, when  $\lambda = 1$ .

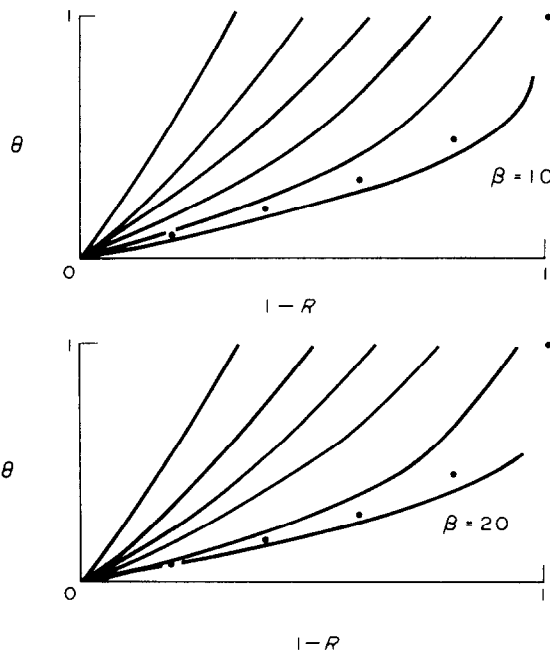


FIG. 4.  $\theta(R)$  at various times  $\beta\tau$  according to the asymptotic theory, with  $\beta = 10, 20$  and  $\lambda = 1$ . The continuous lines are all from (2.10a) except the final profiles which are due to the I-II analysis (e.g. (5.1)). The dots are numerical final profiles transferred from Fig. 3 for comparison. Values of  $\beta\tau$  are as in Fig. 3.

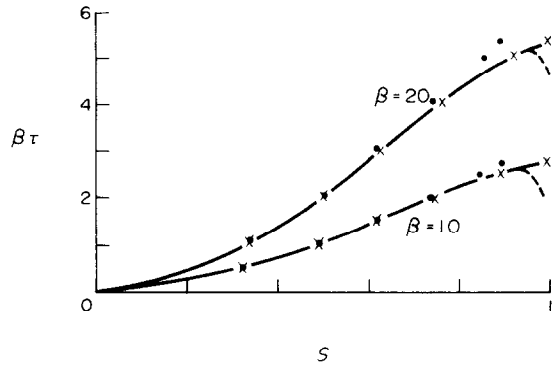


FIG. 5. Front location  $S$  vs time  $\beta\tau$  when  $\beta = 10, 20$  for  $\lambda = 1$ . The crosses are the computations of Beckett [5] and the continuous curves are mainly (2.10b) but with the two-region result (4.9) incorporated near  $S = 1$ . The dashed lines indicate the error in (2.10b) as  $S \rightarrow 1$ .

again (2.10b) is almost identical with the full solutions for nearly all the motion. Lastly, however, near  $S = 1$  the double-structure is called upon to cope with the irregularity in (2.10b), successfully follows the numerical values there and produces the final solidification time

$$\tau_f = \frac{1}{4} + \frac{1}{4\beta} + \frac{1}{4\beta \ln \Delta_1} + \frac{1}{8\beta (\ln \Delta_1)^2} \times \left\{ 16 \sum_{n=1}^{\infty} \frac{\ln j_n}{[J_1(j_n)]^2 \cdot j_n^4} + \gamma - \ln 2 \right\} \quad (5.2)$$

which, if we keep, say, ten terms of the infinite series, is close to the calculated times.

Bearing in mind the asymptotic ( $\beta \rightarrow \infty$ ) nature of the theory, the agreement between it and the numerical solutions of the full equations for  $\beta = 10, 20$  is indeed encouraging, for both thermal and temporal variations. It is noteworthy that, if  $\beta = 10$ ,  $\Delta_1 \approx 0.28$  and the relative order of magnitude of the neglected terms at each stage is  $(-1/\ln \Delta_1)$  or approximately 0.79. Additionally we observe that when (5.2) is taken to just two terms, i.e. if only

$$\tau_f = \frac{1}{4} + \frac{1}{4\beta} \quad (5.3)$$

is used, then we obtain  $\beta\tau_f = 1.25, 2.75, 5.25$  when  $\beta = 4, 10, 20$  as compared with Beckett's results  $\beta\tau_f = 1.19, 2.69, 5.30$  respectively. Thus (5.3) is sufficiently close an approximation for  $\beta \geq 4$  to warrant consideration as a general solidification-time formula for the cylinder, with (5.2) acting to give extra accuracy if desired.

We therefore conclude that, provided the parameter  $\beta$  is large enough, practically all of the freezing process has been described theoretically. The natural development, from series (2.9), (2.10) to the two-region expan-



sions of Section 3, is well illustrated by the comparisons in Figs. 2–5. The one remaining gap in the large- $\beta$  analysis lies well within the region I, in fact in an exponentially small zone of the  $S$ – $R$  plane where the logarithmic behaviour in (4.6a) and (5.1) forces the solutions to become invalid at the last moment. This irregularity requires a further examination to be made very close to  $S = 1$ ,  $R = 0$ . The finer details have not been worked-out, but because of the minute scale involved we may infer that the corrections to our formulae are merely exponentially small ones and so need not be regarded as too significant.

The realization that near the end of the inward solidification process for  $\beta \gg 1$  the principal features in the development of the temperature distribution take place in two separate spatial regions has enabled our understanding to be extended much further towards the ultimate solidification at the centre. The two-tiered phenomenon, wherein the innermost parts of the body are dominated by the required latent heat supply which in turn controls the flow of heat through the rest of the material, evolves because of the relatively fast change in the nature of the process just before solidification is completed, despite the fact that the time-scale of the whole freezing operation is large. The use of the rational theory based on the expansion scheme of Section 3 allows detailed analysis of the double-structure and thereby affords, we believe, more physical insight into the qualitative behaviour of the heat flow. It also indicates that for high  $\beta$  some numerical difficulty might be expected due to the steepness of the temperature profile near solidification and that unless there is some local mesh-refinement accuracy will be lost. The greater  $\beta$  is the more relevant is our work, and Table 1, giving values of  $L/c_p$  for some common metals, shows that  $\beta$  can indeed be

large for realistic temperature differences; in practice if a large temperature difference were set it would not generally remain so because of the heating of the surrounding medium. Our perturbation approach can no doubt be directly applied to give simplistic models of many problems of practical interest, such as the solidification of cylindrical castings or pipes, the cooling of planets and the freezing of hailstones and ballbearings. The model is readily modified to include many other features, e.g. radiation or periodic conditions at the surface, and may well preclude the necessity for extensive computation in more complex situations.

#### REFERENCES

1. L. I. Rubinstein, The Stefan problem, *Trans. Math. Monogr.* **27** (1971) (translated by A. D. Solomon).
2. H. S. Carslaw and J. C. Jaeger, *Conduction of Heat in Solids*. Oxford University Press, Oxford (1959).
3. L. C. Tao, Generalised numerical solutions of freezing a saturated liquid in cylinders and spheres, *A.I.Ch.E. JI* **13**(1), 165 (1967).
4. G. Poots, On the application of integral-methods to the solution of problems involving the solidification of liquids initially at fusion temperature, *Int. J. Heat Mass Transfer* **5**, 525 (1962).
5. P. M. Beckett, Ph.D. Thesis, Hull University (1971).
6. R. I. Pedroso and G. A. Domoto, Perturbation Solutions for spherical solidification of saturated liquids, *J. Heat Transfer* **95**, 42 (1973).
7. R. I. Pedroso and G. A. Domoto, Inward spherical solidification—solution by the method of strained coordinates, *Int. J. Heat Mass Transfer* **16**, 1037 (1973).
8. D. S. Riley, Ph.D. Thesis, Hull University (1972).
9. M. Abramowitz and I. A. Stegun (Editors), *Handbook of Mathematical Functions*. Dover, New York (1965).
10. D. N. de G. Allen and R. T. Severn, The application of the relaxation method to the solution of non-elliptic partial differential equations, *Q. JI Mech. Appl. Math.* **15**, 53 (1962).

#### SOLIDIFICATION INTERNE DE SPHERES ET DE CYLINDRES CIRCULAIRES

**Résumé**—On présente une étude analytique du gel interne d'une sphère ou d'un cylindre circulaire, initialement fondu et à la température de fusion, lorsque la surface externe est brusquement refroidie. Entre autres hypothèses, on suppose que les propriétés thermiques sont constantes et que le paramètre  $\beta$ , rapport de la chaleur latente à la chaleur sensible, est grand. On détermine tout d'abord des solutions séries fondamentales et on dégage une analyse à deux régions qui est utilisée pour tenir compte du brusque changement du profil thermique juste avant que le centre de la sphère ou du cylindre se solidifie. Bien que la théorie soit strictement asymptotique par nature, les résultats s'accordent bien avec les solutions numériques du problème entier pour  $\beta = 10$  et 20 (cylindre) et  $\beta = 10$  (sphère).

#### DER ERSTARRUNGSVORGANG IN KUGELN UND ZYLINDERN

**Zusammenfassung**—Eine analytische Untersuchung befaßt sich mit dem Erstarrungsvorgang in Kugeln oder Kreiszyllindern, wenn bei anfänglich flüssigem Inhalt bei Schmelztemperatur die Außenwand plötzlich gekühlt wird. Bei der Behandlung des Problems werden unter anderem konstante thermische Eigenschaften angenommen und vorausgesetzt, daß die latente Wärme gegenüber der fühlbaren Wärme

groß ist. Um den Knick im Temperaturverlauf im Zentrum der Kugel oder des Zylinders vor dem Erstarren zu erfassen, wird eine Unterteilung in zwei Bereiche vorgenommen. Obwohl die Theorie ein Näherungsverfahren darstellt, stimmen die Ergebnisse gut mit den Resultaten numerischer Rechenverfahren für  $\beta = 10$  und  $20$  (Zylinder) und  $\beta = 10$  (Kugel) überein, wobei  $\beta$  den Quotienten aus latenter Wärme und fühlbarer Wärme darstellt.

#### ЗАТВЕРДЕВАНИЕ ШАРОВ И КРУГОВЫХ ЦИЛИНДРОВ

**Аннотация** — В работе проводится аналитическое исследование затвердевания шара или кругового цилиндра, находящегося сначала в расплавленном состоянии при температуре плавления, наружная поверхность которого внезапно охлаждалась. Наряду с другими допущениями, сделанными в работе, тепловые свойства материала считаются постоянными, а параметр  $\beta$  (отношение скрытой теплоты к осязательной теплоте) принимается большим. Полученные вначале общие решения в виде рядов подвергаются затем анализу для двух областей, необходимому для приведения в соответствие резких изменений температурного профиля непосредственно перед затвердеванием центра шара или цилиндра. Хотя теория сугубо асимптотична по своему характеру, результаты хорошо согласуются с полными численными решениями задачи для  $\beta = 10$  и  $20$  (цилиндр) и  $\beta = 10$  (шар).